Advanced Powder Technology 33 (2022) 103466

Contents lists available at ScienceDirect

Advanced Powder Technology

journal homepage: www.elsevier.com/locate/apt

Original Research Paper

Experimental investigation on the spreadability of cohesive and frictional powder

Wenguang Nan [a,b,*], Yiqing Gu [a]

[a] School of Mechanical and Power Engineering, Nanjing Tech University, Nanjing 211816, China
[b] School of Chemical and Process Engineering, University of Leeds, Leeds LS2 9JT, UK

ARTICLE INFO

Article history:
Received 13 October 2021
Received in revised form 7 December 2021
Accepted 26 January 2022
Available online 9 February 2022

Keywords:
Spreadability
Flowability
Spreading
Additive Manufacturing
Cohesive

ABSTRACT

Spreadability of cohesive and frictional powder is critical in powder spreading of additive manufacturing. Different to flowability, the experimental test techniques and underlying powder mechanics of spreadability have not yet been thoroughly acknowledged. In this work, the effects of operation conditions and particle properties on the spreadability of metal powder are experimentally investigated. A measure of relative spreadability based on D_{90} is proposed, considering the effect of size classes of powder. The results show that the spreadability is a non-monic function of the spreading speed, and there is an optimal spreading speed. A concept of dynamic spreadability is also proposed to consider the demand of a high manufacturing rate in AM. The spreadability is strongly affected by the detachment of particles from the heap and the re-filling process of the depletion region. Excellent spreadability could only be obtained in a specified range of flowability, where the powder should neither extremely cohesive nor excessively free-flowing with little frictional resistance.

© 2022 The Society of Powder Technology Japan. Published by Elsevier B.V. and The Society of Powder Technology Japan. All rights reserved.

1. Introduction

Additive manufacturing (AM) has attracted great attention in recent years in a wide range of industrial applications [1–5]. In the powder-based manufacturing method, the dry powder is spread onto the work surface by a blade or roller spreader to form a thin powder layer with a thickness of a few of particle diameters, and then the powder layer is shone by the laser or electron beams in a scanning mode to melt/sinter a selected area. However, powder used in additive manufacturing is usually fine and cohesive, and it poses great challenges for the spreading process due to the inter-particle attractive and frictional forces. They could cause the formation of empty patches, insufficient amount of powder within the powder layer, and in some particular cases, the powder even could not be spread through the narrow spreading gap [6,7]. Therefore, an in-depth understanding of the spreadability of the cohesive and frictional powder flowing through a narrow spreading gap is helpful for further development of this technology and introduction of new materials.

Although various work has addressed the effects of operation conditions and particle properties on the powder spreading process by Discrete Element Method (DEM) [8–17], there are limited experimental techniques and no standard test methods so far to assess powder spreadability for AM. Flowability of powder used in AM has been widely characterised [18–21] using the devices for bulk cohesive powder flow [7,22,23] (e.g. FT4 Powder Rheometer, Granudurm), but flowability is not the measure of spreadability [6,7]. The detailed definition of spreadability is firstly proposed by Nan et al. [6] and Ghadiri et al. [7], which is given as the ability of the powder to be spread uniformly as a thin layer of a few multiples of particle size without the formation of any empty patches, presence of agglomerates and rough surfaces. They also clarified spreadability and flowability are two different measures of powder flow characteristics, albeit inter-related. However, till now, only a few of work is related to the spreadability of cohesive and frictional powder in AM. Snow et al. [24] attempted to establish powder spreadability metrics by comparing the fraction of powder coverage of the build plate, the rate of powder deposition, the average avalanching angle of the powder heap, and the rate of change of the avalanching angle. Ahmed et al. [25] developed a criterion for describing the powder spreadability by using the size and frequency of empty patches. They proposed a simple and quick method to quantitatively access the spreadability of 316L stainless steel powder based on the image analysis, where the spread layer was re-constructed by several segmented SEM images through image processing. Although spreadability was also mentioned in

* Corresponding author at: School of Mechanical and Power Engineering, Nanjing Tech University, Nanjing 211816, China.
E-mail address: nanwg@njtech.edu.cn (W. Nan).

https://doi.org/10.1016/j.apt.2022.103466
0921-8831/© 2022 The Society of Powder Technology Japan. Published by Elsevier B.V. and The Society of Powder Technology Japan. All rights reserved.

Cordova et al. [26], it mainly focused on the flowability of cohesive powder while the details of spreadability were not detailed reported. Mussatto et al. [27] analysed the effects of powder morphology and spreading parameters on the spreadability, which was described by profile height and profile void volume measured from powder bed topography, but no criterion was proposed to compare the relative spreadability of different powder. Shaheen et al. [28] explored the influence of materials and process parameters on the layer quality, and they showed that increasing the spreading speed could decrease the layer quality for both non– and weakly cohesive powders whilst improve the layer quality for strongly cohesive powder. Le et al. [29] proposed a method to assess powder bed quality as a function of both powder conditions and recoating strategies based on powder bed scanner technology, which offers a new opportunity to explore the spreadability of powder materials to optimise PBF processes.

In this work, the spreadability of cohesive and frictional powder is experimentally reported. A criterion is proposed to quantify the spreadability of powder with different materials and size classes. The effects of the operation conditions and particle properties on the spreadability are analysed, and the underlying mechanisms are also investigated. The difference between the spreadability and flowability is also clarified based on the experimental results. This provides a further step towards understanding the spreadability of powder in additive manufacturing, and it also provides a reference to validate powder spreading simulations.

2. Materials and methods

Three kinds of metal powder in additive manufacturing are used here: 15–53 μm 316L stainless steel powder, 15–53 μm AlSi10Mg powder, and 1–15 μm 316L stainless steel powder. They have been widely used in the commercial machines of additive manufacturing. It should be noted that 15–53 μm and 1–15 μm here are the product label, which do not accurately represent the real particle size range of the powder. For convenience, they are assigned as powder A, B, C, respectively. The number-based and volume-based particle size distribution is shown in Fig. 1, with D_{10}, D_{50} and D_{90} shown in Table 1, which is measured by the Malvern Mastersizer 2000, and the SEM images are shown in Fig. 2. According to previous work [6,7,25,30–32], the number-based D_{90} is used as the characteristic particle size, which is 32.7 μm, 37.6 μm and 13.4 μm for powder A, B and C, respectively. The flowability of powder is examined by Hall Flow Tester (i.e. opening size of 2.5 mm) based on the test procedure of ASTM B213. The flow rate of powder A is 19 s /50 g, whilst no flow could be observed for C. For powder B, the flow is interrupted after a small amount of powder flowing out the funnel. The flowability of powder is also examined by the static repose angle. It is measured from the fixed funnel method, in which a fixed mass of the powder is poured through a funnel with an opening size of 5 mm. For powder B and C, the powder is gently stirred to facilitate flowing out the funnel. The static repose angle of these three kinds of powder is 31°, 39° and 49°, respectively, as shown in Table 1. Thus, according to Table 1, powder A is slightly cohesive, and powder B and powder C are moderately cohesive and very cohesive, respectively. The particle density is shown in Table 1, which is provided by the powder suppliers.

The experiment rig is shown in Fig. 2, mainly comprising of a baseplate, blade, linear servo motor, and accessories. The gap height between the blade tip and baseplate is precisely controlled by a lifting platform with a micrometre calliper, and a feeler gauge. The flatness of the baseplate is ± 20 μm. The blade moves at a constant velocity, which is controlled by a linear servo motor with high accuracy. Four gap heights are used in this work, i.e. δ = 50,

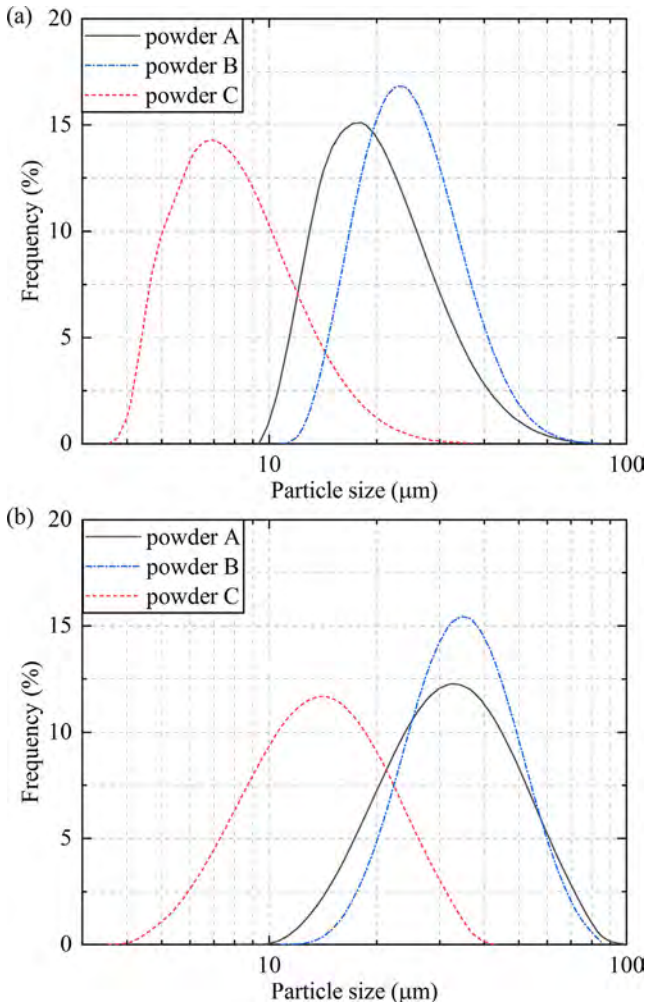

Fig. 1. Particle size distribution of the powder: (a) number-based, and (b) volume-based.

100, 150 and 200 μm. The gap height is controlled by the feeler gauge before spreading, and it is also re-examined after the spreading using the same method. For each gap height, six spreading speeds are adopted, i.e. U = 0.001, 0.01, 0.04, 0.08, 0.12 and 0.16 m/s. For each spreading condition, three repetitive experiments are carried out and the averaged results are used. The powder is fed into a rectangular slot by a micro-vibration feeder and then the slot is removed upwards to form a powder pile in the preparation area naturally. After removing the slot, the powder heap is spread onto the baseplate by a 316L stainless steel blade. After slightly removing the strips along with the baseplate, the baseplate is taken out carefully, and the spread layer on the baseplate is brushed down and weighed by a balance with a precision of 0.01 g. In this work, the powder is dried before and after each test, in which the effect of moisture during storage and spreading process could be minimised.

3. Results

According to the work of Nan et al. [6], Ghadiri et al. [7] and Ahmed et al. [25], powder spreadability is defined as the ability of powder passing through the gap and being spread uniformly as a thin layer of a few multiples of particle size without the formation of any empty patches, presence of agglomerates and rough surfaces. Based on this concept, two methods could be used to

Table 1
Physical properties of the metal powder used in the experiment.

Powder	Material	Density (g/cm^3)	Volume-based D_{10}, D_{50}, D_{90} (μm)	Number-based D_{10}, D_{50}, D_{90} (μm)	Repose angle (°)	Standard deviation of repose angle	Flow rate
A	316L stainless steel	7.9	18.5, 32.3, 55.3	13.0, 19.3, 32.7	31	1.33	19 s/50 g
B	AlSi10Mg	2.67	22.2, 34.6, 53.5	16.6, 24.2, 37.6	39	0.92	–
C	316L stainless steel	7.9	7.6, 13.7, 24.0	5.0, 7.7, 13.4	49	1.69	–

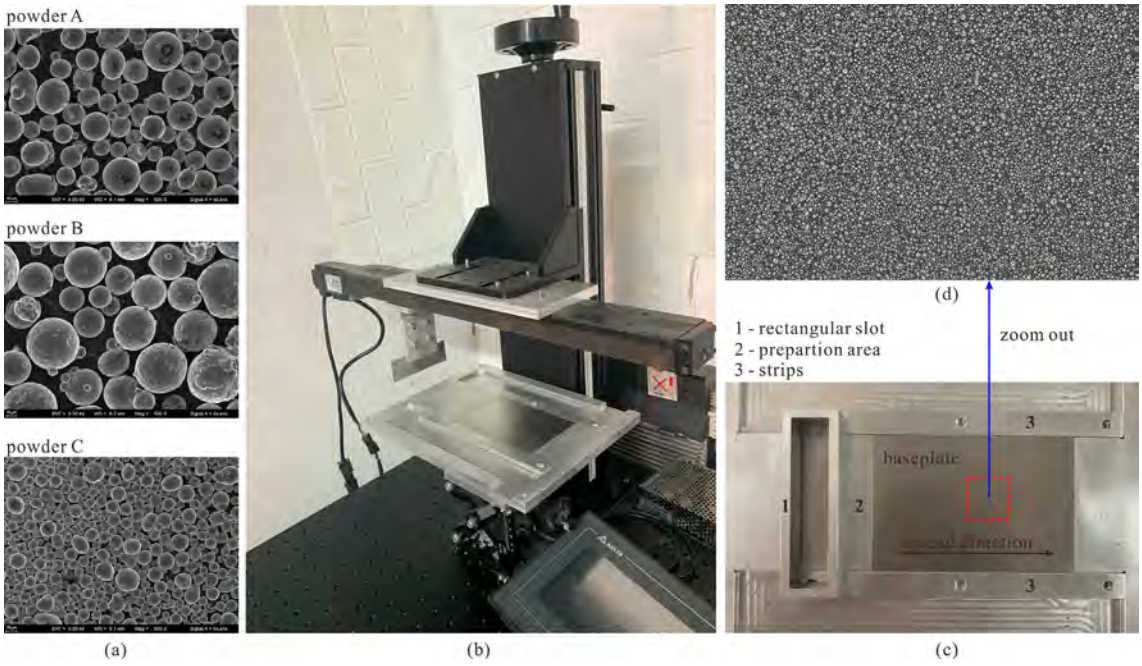

Fig. 2. Experiment system in this work: (a) SEM images of powder; (b) snapshot of the experiment rig; (c) work surface; (d) spread layer.

quantify the spreadability of powder in additive manufacturing, i.e. image/morphology analysis of the empty patches within the spread layer, and the normalised mass of the spread layer. The first method is attractive, but it is usually limited to a small area of the spread layer [25,27] due to the small visual field in microscope or SEM or x-ray technique, thus, it may be not representative of the whole spread layer. Although the splicing technique of segmented images could be adopted to get a larger visual field as used in Ahmed et al. [25], the post-processing and analysis of the images are complex. Contrarily, the second method is simple and also quick, although it is less accurate than the first method. In this work, the second method (i.e. the normalised mass of the spread layer) is used. The spreadability *(SP)* is defined in Eq. (1), and the spreadability between different powder could be compared by plotting *SP* with δ/D_{90}:

$$SP = \frac{M}{\rho LWD_{90}} \tag{1}$$

where M is the measured total mass of the particles within spread layer; L is the length of the spread layer (i.e. in the spread direction); W is the width of the spread layer; ρ is the particle density, as shown in Table 1. The adoption of D_{90} in Eq. (1) is based on the analysis in our previous work [6,7,25,30–32], where more details could be found. It should be noted that the spreadability defined in Eq. (1) does not indicate a definite value for a specified powder, and its exact value depends on the spreading conditions, such as spreading speed and gap height. Therefore, it is only used to determine the spreadability of specified powder relative to a standard powder. It should be noted that the relative spreadability of different powders should be compared at the same ratio of the gap height to particle size (i.e. δ/D_{90}) instead of gap height. Taking an extreme case as an example, at very small gap height, e.g. 50 μm, finer particles (e.g. 15–53 μm) usually could get a better spread layer than the ones with a larger size class (e.g. 53–106 μm), but it is due to the size effect (e.g. 53–106 μm could not even pass through the gap) instead of good spreadability. This is also one of the reasons that D_{90} is used in Eq. (1) for normalisation instead of the gap height.

The variation of the spreadability with spreading speed is shown in Fig. 3. For all kinds of powder and spreading gap heights in the experiment, almost the same trend is observed. With the increase of spreading speed, spreadability increases first and then decreases. Therefore, there is an optimal spreading speed, at which a maximum spreadability is obtained. This non-monotonic trend has not been found in previous DEM simulations [30], where the cases with low spreading speed (e.g. 0.01 m/s) are usually not involved. To depict the underlying mechanisms of this non-monotonic relationship between spreadability and spreading speed, the spreading state is divided into two regimes based on the optimal spreading speed: regime I and regime II. In the former, the spreading speed is less than the optimal spreading speed, for which the spreadability increases with the spreading speed, and in the latter, it is in the opposite situation.

In regime I (i.e. spreading speed is lower than the optimal speed), the shearing strain rate is small. At extremely low spreading speed (e.g. U = 0.001 m/s), the shearing strength of the blade on the heap is not enough to counteract the adhesion between particles. Due to the attractive tensile force, the particles are adhered to each other, and the powder heap is pushed forward like a moving block. Thus, the powder close to the blade tip cannot be freely

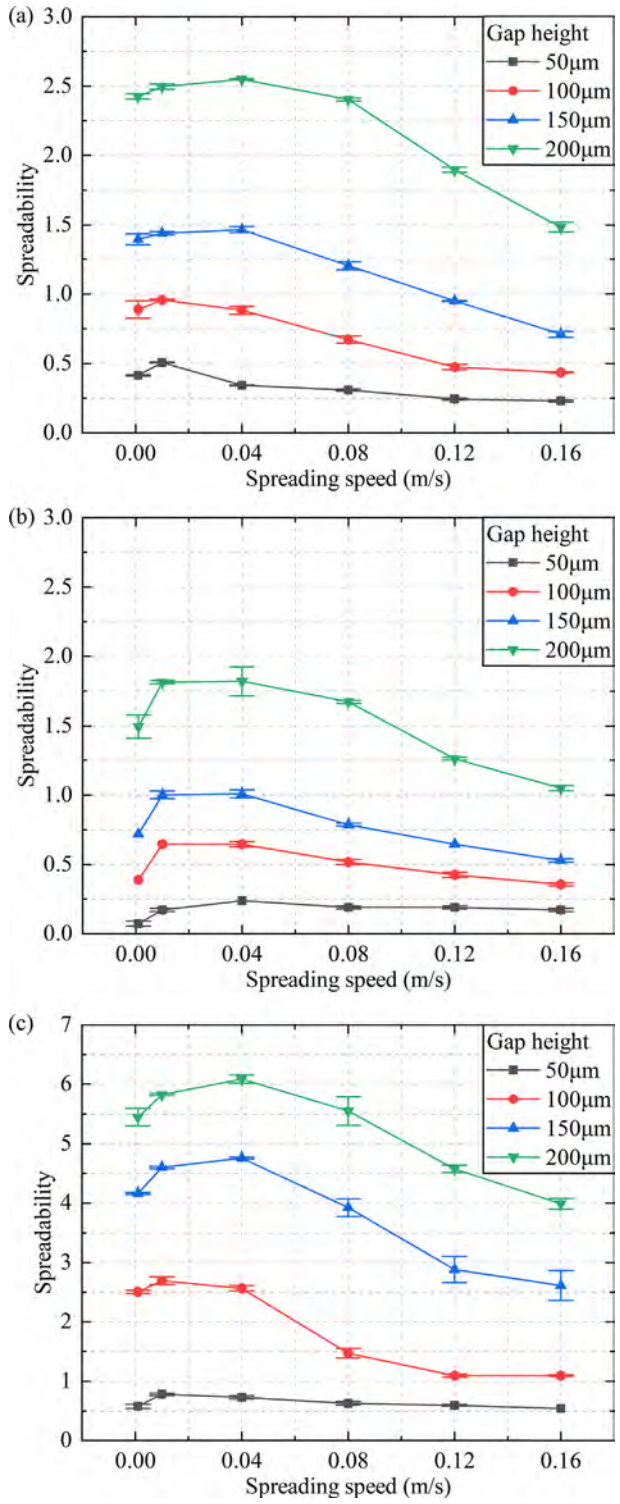

Fig. 3. Variation of the spreadability with the spreading speed: (a) powder A, (b) powder B and (c) powder C.

sheared, and there is no enough powder being sheared down and detached from the heap. As the spreading speed increases, the shearing strength of the blade on the heap is enhanced, resulting in enough powder being able to be spread onto the baseplate, and thus the spreadability is improved. For example, compared to powder A, the adhesion between particles in powder B is stronger, resulting in a larger difference of spreadability between U = 0.001 m/s and U = 0.01 m/s, which is intuitively expected based on this mechanism.

In regime II (i.e. spreading speed is higher than the optimal speed), the shearing strain rate is very large. The particle dynamics in the powder heap are mainly dominated by the shearing effect of the blade. With the increase of spreading speed, blade shearing action is enhanced, resulting in two major effects: more prone to transient jamming especially for small gap height, and larger inertia of particles within the heap in the spreading direction. In the former, the particle flow through the gap is transiently interrupted, resulting in a decrease of the amount of powder spread onto the baseplate. In the latter, the expending of particles at the space close to the blade as they are spread onto the baseplate, could not be immediately replenished by the upper particles falling down under gravity, resulting in fewer particles that could further spread onto the baseplate. Both effects could lead to a decrease of spreadability with the increase of the spreading speed.

As shown in Fig. 3, the maximum value of spreadability could be obtained at the spreading speed of U = 0.01–0.04 m/s, which depends on particle properties and spreading conditions. For example, for powder A, the maximum value of spreadability occurs at U = 0.01 m/s for gap height of δ = 100 μm whilst U = 0.04 m/s for gap height of δ = 200 μm. However, in reality, a larger spreading speed is usually demanded to speed up the manufacturing process. Based on this point, the spreadability in Eq. (1) could be further extended to the dynamic spreadability, namely, the ability of getting the spread layer with good quality in a short time, which could be given as:

$$SP_d = SP \times U \tag{2}$$

As shown in Fig. 4, with the increase of the spreading speed, the dynamic spreadability for powder A and B increases firstly and then approaches to a plateau. Considering the spreading efficiency in the manufacturing process, the optimum spreading speed could be defined as the speed at which the dynamic spreadability starts to approaches to a plateau with the increase of spreading speed. For powder A and B, the optimum spreading speed is between 0.08 and 0.12 m/s. It agrees well with the suggested value (i.e. 0.1 m/s) in Nan et al. [30].

As shown in Fig. 3, the spreadability is also significantly affected by the spreading gap height, which is re-plotted at the spreading speed of 0.08 m/s in Fig. 5. For powder A and B, with the increase of the gap height, the spreadability first increases almost linearly, and then it shows a sharp increase as the gap height is increased to 200 μm, as the wall effect of the baseplate on the particle flow in the gap region is minimised at this gap height among all cases in this work. For powder C, the spreadability shows a larger value than powder A and B, but it is due to the size effect (smaller D_{90} in Eq. (1) and also smaller boundary effect of the baseplate wall on the particle flow in the gap region). It again suggests that the relative spreadability of powder with different size classes should be compared at the same ratio of the gap height to particle size instead of at the same gap height.

4. Discussions

4.1. Factors affecting spreadability

Based on the above analysis, the spreading process of powder onto the baseplate could be divided into three stages: detachment of particles from the heap, re-filling of the depletion region by its surrounding particles, particle flowing through the gap region, as shown in Fig. 6. The spreadability is affected by the particle dynamics in these stages:

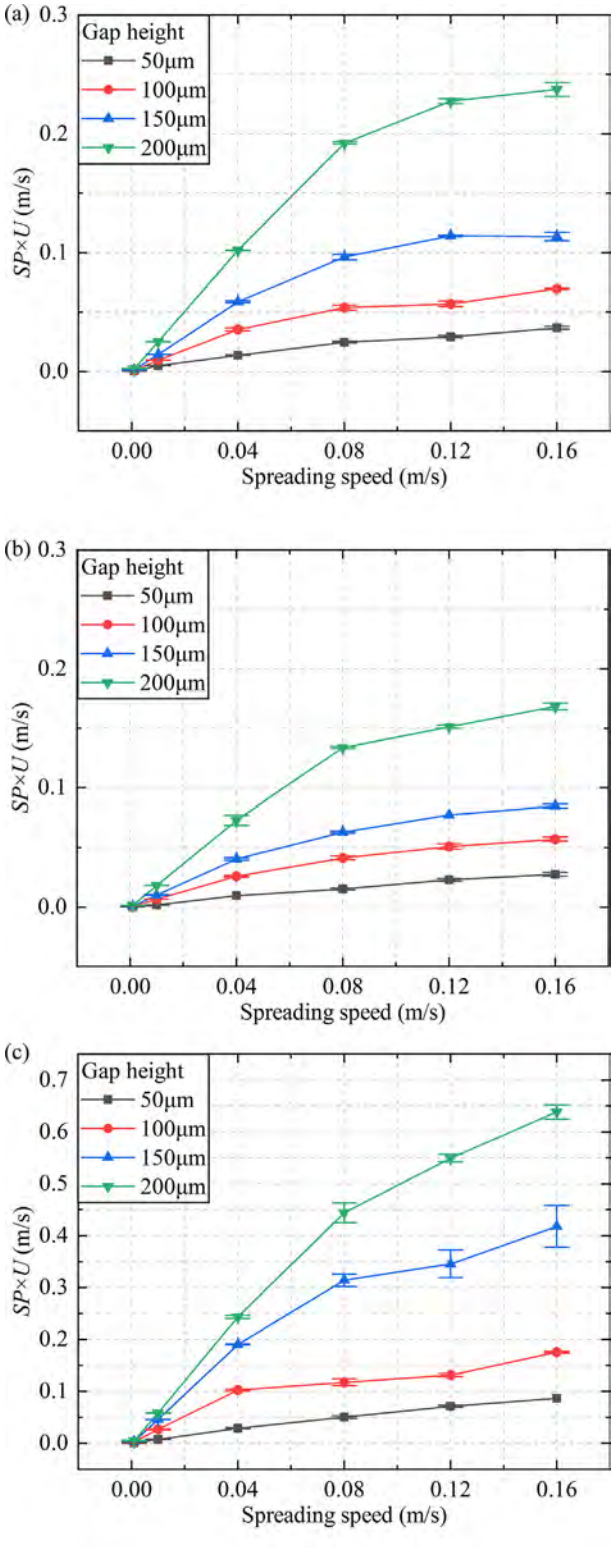

Fig. 4. Variation of the dynamic spreadability ($SP \times U$) with the spreading speed: (a) powder A, (b) powder B and (c) powder C.

More easily the detachment of particles from the heap indicates more particles being able to enter into the gap region. The detachment of particles is mainly affected by the blade shearing on the heap and the adhesion between the particles and the heap. If the particles are very cohesive, they would be adhered to each other

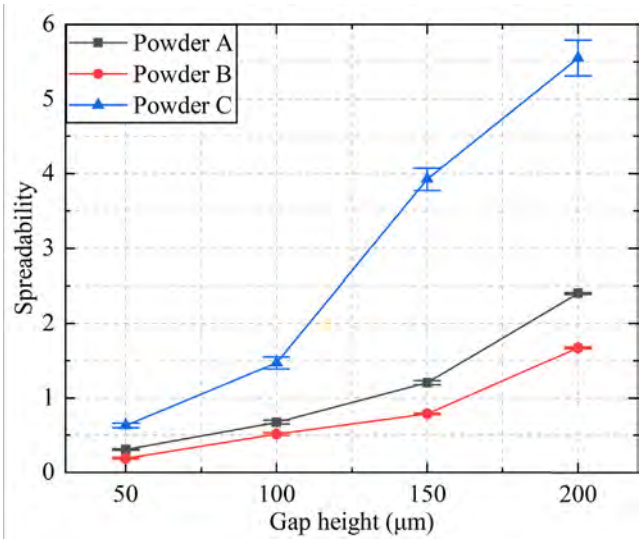

Fig. 5. Variation of the spreadability with the gap height at the spreading speed of 0.08 m/s.

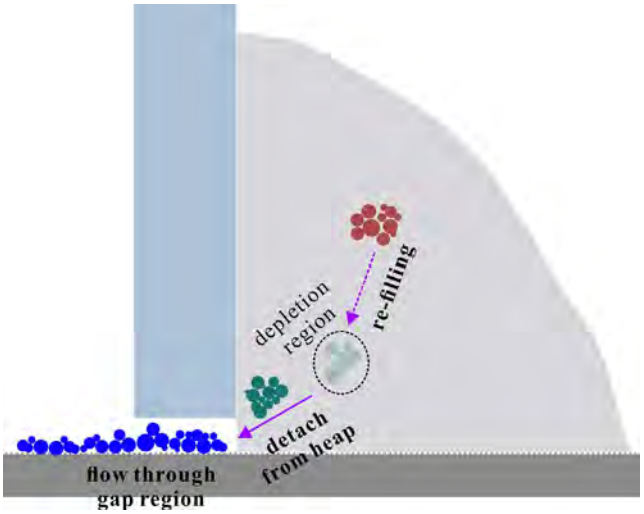

Fig. 6. Illustration of the spreading process at single-particle scale.

like a paste and could not detach from the heap if the blade shearing is also weak (very small spreading speed). In this situation, the particles in front of the blade move like a slug, resulting in a very low spreadability.

The sustainability of the detaching stage is affected by the re-filling stage. The detaching of particles from the heap would result in a depletion region in front of the blade. As reported by Nan et al. [31], in the blade spreading process, the convection/circulation of particles within the heap is very weak, thus, the re-filling process is mainly driven by gravity and gravity-indcued contact force. If the blade spreading speed is very high, i.e. $U \gg (gD_{90})^{0.5}$ [31], the re-filling rate under gravity is less than the depletion rate. In this case, the depletion region due to detachment could not be immediately re-filled by the surrounding particles, and the detachment would not be sustainable. Therefore, the amount of particles detached from the heap would auto-decrease to achieve a balance between the re-filling rate and depletion rate.

The sustainability of the detaching stage is also affected by the particles flowing through the gap region. Less velocity of particles flowing through the gap region, indicates a larger velocity

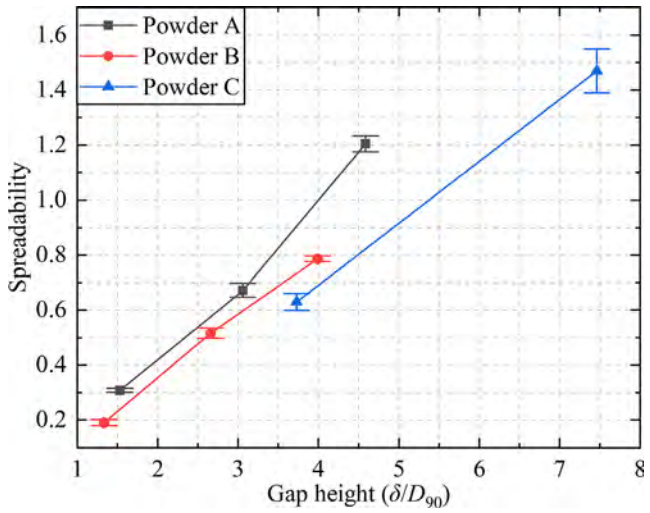

Fig. 7. Comparison of the spreadability between different powders at the spreading speed of 0.08 m/s.

Table 2
Physical properties of the glass beads for comparison.

	D_{10} (μm)	D_{50} (μm)	D_{90} (μm)	Repose angle (°)
Slight-cohesive	47	63	89	28
Free-flowing	241	327	472	23

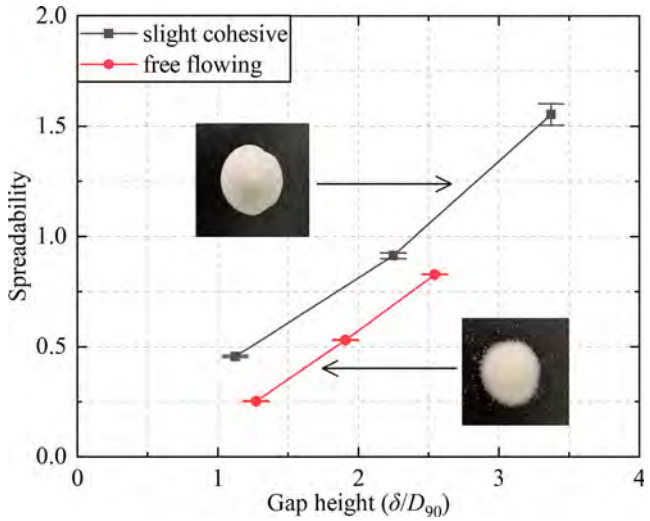

Fig. 8. Comparison of the spreadability between free-flowing and slight-cohesive glass beads at the spreading speed of 0.08 m/s.

difference between the spreader and particles. In this case, the particles could be more quickly left away from the blade, i.e. the gap region could be more quickly emptied to leave space for the detached particles entering into the gap. If not considering particular cases, the particles usually are not in contact with the blade in the gap region, thus, particle velocity in the gap region is mainly determined by the initial particle inertial when detaching from the heap. Frictional resistance due to baseplate and particle–particle interaction also has effects on the particle velocity, but the effects are usually minor due to the small length of gap region. Compared to the detaching and re-filling stages, the effect of particles passing through the gap region on the spreadability is smaller.

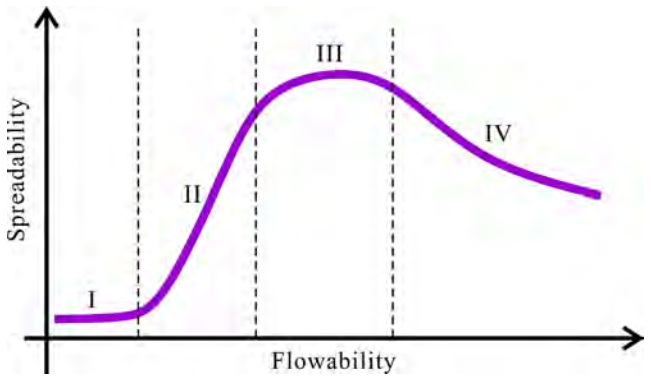

Fig. 9. Schematics of the variation of spreadability with flowability: zone I- powder is too cohesive to be spread by the blade spreader; zone II: powder is moderate-cohesive, where the spreadability could be significantly improved by enhancing the flowability; zone III: powder with slight cohesion or interlocking due to particle shape, where excellent spreadability could be obtained; zone IV: free-flowing with little frictional resistance, where spreadability is slightly reduced with further increase of flowability.

However, it may also have a significant effect on the spreadability, if particle jamming occurs in the gap region, or the roller spreading with strong particle-gas interaction is considered [32].

With the increase of powder cohesion, the detachment of particles by the blade shearing is reduced, the re-filling rate of the depletion region is also slow down, thus, the spreadability is reduced. It could be found Fig. 7, where the spreadability of powder A-C at the spreading speed of U = 0.08 m/s is compared at different gap heights, which are normalised by D_{90}. Similarly, with the increase of the gap height, the shearing strength on the heap is enhanced, resulting in a large amount of particles detached from the heap and thus an increase of spreadability, as shown in Fig. 5. With the increase of spreading speed, the detaching process is enhanced but the re-filling process is weakened, thus, there would be a competition between these two processes, resulting in an optimal spreading speed, as shown in Fig. 3.

4.2. Spreadability and flowability

Spreadability is significantly affected by flowability to some extent, however, they are different measures of powder flow characteristics, as previously clarified by Ghadiri et al. [7] and Nan et al. [32]. Flowability mainly affects the detachment of particles from the heap and the re-filling of the depletion region in Fig. 6, where the particle flow is in the form of bulk flow. However, the spreadability is also affected by the particle flow in the gap region, which is in the form of thin-layer flow with significantly discrete features, such as the particle jamming in the narrow spreading gap [6] and the gas effect in roller spreading for very fine powder [32]. Here, another special case is reported here to experimentally validate the difference between spreadability and flowability. Instead of using better metal powder (e.g. excellent good sphericity and optimised particle size distribution) at high cost, two kinds of glass beads are used as reference materials to illustrate the difference between flowability and spreadability, and larger particle size (less cohesion) is used to enlarge this difference. The physical properties of the glass beads are shown in Table 2, with number-based D_{90} of 89 and 472 μm, respectively. One is slight-cohesive and the other one is free-flowing, with the repose angle of 28° and 23°, respectively. The spreadability of these two kinds of powder is compared in Fig. 8, where only part of results is shown here for a clear spot while not affecting the conclusions. It is clear that the spreadability of the free-flowing glass beads is worse than that of the slight-cohesive glass beads. For the free-flowing glass beads, the particle

inertial is large, and they are not easy to pack as a thin layer under gravity effect due to their spherical shape with less flow resistance. It may be also attributed to other effects, which need further investigation in future. However, it should be noted that the spreadability in Fig. 8 is still better than that shown in Fig. 7. Therefore, to gain a better spreadability, the powder should not be too free-flowing, and the powder with slight cohesion or interlocking due to particle shape is more attractive.

Based on the above discussion, a general variation of spreadability with flowability could be empirically summarised and schematically shown in Fig. 9, which may need further investigation in future. For convenience, it is classified into four zones. If the flowability is very worse (i.e. zone I), the powder could even not be spread onto the baseplate due to the strong adhesion force between particles and also the agglomerations. In this case, the blade spreader is not suitable anymore, and a roller spreader with a large rotational speed is attractive. Thus, to spread the powder onto the baseplate by using a blade spreader, the flowability should be above the critical value. With the increase of the flowability, the spreadability increases first (i.e. zone II, e.g. metal powder A-C in this experiment) and then approaches to a plateau (i.e. zone III, e.g. slightly cohesive glass beads in this experiment), where the spreadability varies little with the flowability. With further increase of the flowability (i.e. zone IV, e.g. free-flowing glass beads with little frictional resistance in this experiment), the spreadability is slowly reduced. Therefore, to get an excellent spreadability, the flowability should be controlled in a specified range, where the powder should neither be extremely cohesive nor excessively free-flowing with little frictional resistance.

5. Conclusion

The spreadability of cohesive and frictional powder is experimentally reported in this work. The effects of the operation conditions and particle properties on the spreadability are analysed, and the underlying mechanisms are also investigated. The difference between the spreadability and flowability is also clarified based on the experimental results. The main results from the present study are summarised as follows:

1) A measure of spreadability is proposed for powder with different size classes, where the normalised mass of the spread layer is plotted against the gap height divided by D_{90}. A concept of dynamic spreadability is also proposed considering the demand of a high manufacturing rate in additive manufacturing. The relative spreadability of powder with different size classes should be compared at the same ratio of the gap height to particle size instead of at the same gap height.
2) Spreadability is usually affected by three stages in the spreading process: detaching of particles from the heap, re-filling of the depletion region by its surrounding particles, particle flowing through the gap region.
3) With the increase of spreading speed, there would be a competition between the detaching and re-filling processes, resulting in an optimal spreading speed. With the increase of powder cohesion, the spreadability is usually reduced due to less detachment of particles from the heap and slow re-filling rate of the depletion region, if not considering particular cases.
4) Spreadability is significantly affected by flowability to some extent, but they are different measures of powder flow characteristics. Excellent spreadability could only be obtained in a specified range of flowability, where the powder should neither be extremely cohesive nor excessively free-flowing with little frictional resistance

Declaration of Competing Interest

The authors declare that they have no known competing financial interests or personal relationships that could have appeared to influence the work reported in this paper.

Acknowledgments

The authors are grateful to the National Natural Science Foundation of China (Grant No. 51806099) for the financial support of this work. The second auhor is grateful to Jiangsu Province Postgraduate Practice Innovation Program (Grant No. SJCX21_0492) for the financial support. The first author is also thankful to Professor Mojtaba Ghadiri, University of Leeds, UK, and Professor Yueshe Wang, Xi'an Jiaotong University, China, for the inspiration and encouragement on this work.

References

[1] C.W. Foster, H.M. Elbardisy, M.P. Down, E.M. Keefe, G.C. Smith, C.E. Banks, Additively manufactured graphitic electrochemical sensing platforms, Chem. Eng. J. 381 (2020) 122343, https://doi.org/10.1016/j.cej.2019.122343.
[2] E. Miramontes, L.J. Love, C. Lai, X. Sun, C. Tsouris, Additively manufactured packed bed device for process intensification of CO2 absorption and other chemical processes, Chem. Eng. J. 388 (2020) 124092, https://doi.org/10.1016/j.cej.2020.124092.
[3] K.R. Ryan, M.P. Down, C.E. Banks, Future of additive manufacturing: Overview of 4D and 3D printed smart and advanced materials and their applications, Chem. Eng. J. 403 (2021).
[4] S.F. Shirazi, S. Gharehkhani, M. Mehrali, H. Yarmand, H.S. Metselaar, N. Adib Kadri, N.A. Osman, A review on powder-based additive manufacturing for tissue engineering: selective laser sintering and inkjet 3D printing, Sci Technol, Adv Mater 16 (2015) 033502.
[5] I. Gibson, D. Rosen, B. Stucker, Additive manufacturing technologies, 3D printing, rapid prototyping, and direct digital manufacturing, Springer, New York, 2015.
[6] W.G. Nan, M. Pasha, T. Bonakdar, A. Lopez, U. Zafar, S. Nadimi, M. Ghadiri, Jamming during particle spreading in additive manufacturing, Powder Technol. 338 (2018) 253–262.
[7] M. Ghadiri, M. Pasha, W.G. Nan, C. Hare, V. Vivacqua, U. Zafar, S. Nezamabadi, A. Lopez, M. Pasha, S. Nadimi, Cohesive Powder Flow: Trends and Challenges in Characterisation and Analysis, Kona Powder Part. J. 37 (2020) 3–18.
[8] Y. He, A. Hassanpour, A.E. Bayly, Linking particle properties to layer characteristics: Discrete element modelling of cohesive fine powder spreading in additive manufacturing, Addit. Manuf. 36 (2020) 101685.
[9] H. Chen, Q.S. Wei, Y.J. Zhang, F. Chen, Y.S. Shi, W.T. Yan, Powder-spreading mechanisms in powder-bed-based additive manufacturing: Experiments and computational modeling, Acta Mater. 179 (2019) 158–171.
[10] H. Chen, Q.S. Wei, S.F. Wen, Z.W. Li, Y.S. Shi, Flow behavior of powder particles in layering process of selective laser melting: Numerical modeling and experimental verification based on discrete element method, Int J Mach Tool Manu 123 (2017) 146–159.
[11] S. Haeri, Optimisation of blade type spreaders for powder bed preparation in Additive Manufacturing using DEM simulations, Powder Technol. 321 (2017) 94–104.
[12] S. Haeri, Y. Wang, O. Ghita, J. Sun, Discrete element simulation and experimental study of powder spreading process in additive manufacturing, Powder Technol. 306 (2016) 45–54.
[13] D. Yao, X. An, H. Fu, H. Zhang, X. Yang, Q. Zou, K. Dong, Dynamic investigation on the powder spreading during selective laser melting additive manufacturing, Addit. Manuf. 37 (2021) 101707.
[14] J. Zhang, Y. Tan, T. Bao, Y. Xu, X. Xiao, S. Jiang, Discrete Element Simulation of the Effect of Roller-Spreading Parameters on Powder-Bed Density in Additive Manufacturing, Materials 13 (2020) 2285.
[15] C. Meier, R. Weissbach, J. Weinberg, W.A. Wall, A.J. Hart, Critical influences of particle size and adhesion on the powder layer uniformity in metal additive manufacturing, J. Mater. Process. Technol. 266 (2019) 484–501.
[16] E.J.R. Parteli, T. Pöschel, Particle-based simulation of powder application in additive manufacturing, Powder Technol. 288 (2016) 96–102.
[17] H.W. Mindt, M. Megahed, N.P. Lavery, M.A. Holmes, S.G.R. Brown, Powder Bed Layer Characteristics: The Overseen First-Order Process Input, Metallurgical and Materials Transactions a-Physical Metallurgy and Materials, Science 47 (8) (2016) 3811–3822.
[18] E.R.L. Espiritu, A. Kumar, A. Nommeots-Nomm, J.A.M. Lerma, M. Brochu, Investigation of the rotating drum technique to characterise powder flow in controlled and low pressure environments, Powder Technol. 366 (2020) 925–937.

[19] D. Ruggi, M. Lupo, D. Sofia, C. Barrès, D. Barletta, M. Poletto, Flow properties of polymeric powders for selective laser sintering, Powder Technol. 370 (2020) 288–297.
[20] A.B. Spierings, M. Voegtlin, T. Bauer, K. Wegener, Powder flowability characterisation methodology for powder-bed-based metal additive manufacturing, Progress in Additive Manufacturing 1 (1-2) (2016) 9–20.
[21] J. Zegzulka, D. Gelnar, L. Jezerska, R. Prokes, J. Rozbroj, Characterization and flowability methods for metal powders, Sci Rep 10 (2020) 21004.
[22] M. Tirapelle, A.C. Santomaso, C. Hare, Dynamic ball indentation for powder flow characterization, Powder Technol. 360 (2020) 1047–1054.
[23] R. Freeman, Measuring the flow properties of consolidated, conditioned and aerated powders — A comparative study using a powder rheometer and a rotational shear cell, Powder Technol. 174 (2007) 25–33.
[24] Z. Snow, R. Martukanitz, S. Joshi, On the development of powder spreadability metrics and feedstock requirements for powder bed fusion additive manufacturing, Addit. Manuf. 28 (2019) 78–86.
[25] M. Ahmed, M. Pasha, W.G. Nan, M. Ghadiri, A simple method for assessing powder spreadability for additive manufacturing, Powder Technol. 367 (2020) 671–679.
[26] L. Cordova, T. Bor, M. de Smit, M. Campos, T. Tinga, Measuring the spreadability of pre-treated and moisturized powders for laser powder bed fusion, Addit. Manuf. 32 (2020) 101082, https://doi.org/10.1016/j.addma.2020.101082.
[27] A. Mussatto, R. Groarke, A. O'Neill, M.A. Obeidi, Y. Delaure, D. Brabazon, Influences of powder morphology and spreading parameters on the powder bed topography uniformity in powder bed fusion metal additive manufacturing, Addit. Manuf. 38 (2021) 101807, https://doi.org/10.1016/j.addma.2020.101807.
[28] M.Y. Shaheen, A.R. Thornton, S. Luding, T. Weinhart, The influence of material and process parameters on powder spreading in additive manufacturing, Powder Technol. 383 (2021) 564–583.
[29] T.-P. Le, X. Wang, K.P. Davidson, J.E. Fronda, M. Seita, Experimental analysis of powder layer quality as a function of feedstock and recoating strategies, Addit. Manuf. 39 (2021) 101890, https://doi.org/10.1016/j.addma.2021.101890.
[30] W.G. Nan, M. Ghadiri, Numerical simulation of powder flow during spreading in additive manufacturing, Powder Technol. 342 (2019) 801–807.
[31] W.G. Nan, M. Pasha, M. Ghadiri, Numerical simulation of particle flow and segregation during roller spreading process in additive manufacturing, Powder Technol. 364 (2020) 811–821.
[32] W.G. Nan, M. Pasha, M. Ghadiri, Effect of gas-particle interaction on roller spreading process in additive manufacturing, Powder Technol. 372 (2020) 466–476.